

Optimization of avocado seed nanoparticle extract (ASNE) as green inhibitor on API X65 steel corrosion using response surface methodology

Alice Alao^{1*}, Abimbola Popoola¹, and Modupeola Dada¹

¹Department of Chemical, Metallurgical, and Materials Engineering, Tshwane University of Technology, South Africa.

Abstract. The use of natural products as inhibitors has become increasingly popular due to environmental concerns and the need for sustainable corrosion solutions. In this investigation, response surface methodology (RSM) was utilized to optimize the process variable of ASNE on API X65 steel in 1M HCl acid solution through gravimetric and surface analysis. The influence of concentration, temperature, and exposure time on the inhibition efficiency of avocado seed nanoparticle extract (ASNE) was examined using a central composite design (CCD). The optimum values obtained for the highest inhibition of 95.7% were a temperature condition of 25 °C, a concentration of 5 g/L, and exposure time of 24 hours. Microstructural examination of the studied samples showed a significant surface difference, confirming the formation of a protective layer on the steel surface. Experimental data was in good agreement with the model hence, the study provides valuable insights into the use of ASNE as an inhibitor for API X65 steel and demonstrates the effectiveness of RSM in optimizing the inhibition process variables.

1 Introduction

In the oil and gas industry, the application of different techniques has been used to mitigate corrosion and prolong the lifespan of equipment and pipelines [1]. These techniques include chemical inhibition, blending of product fluids, upgrading materials, and process control in an effort to mitigate carbon steel corrosion. The use of acidic solutions for petrochemical processes, oil well acidification, and industrial cleaning is very common. Among the several techniques for corrosion prevention and control, corrosion inhibitor is one of the cheapest means, particularly in acid media such as acetic, phosphoric, sulphuric, HCl, and nitric acids [2]. Inhibitor is utilized in different systems, such as oil and gas production, boilers, refinery units, chemicals, and cooling systems. The majority of efficient inhibitor heteroatoms feature such as S, N, and O, as well as many bonds in their molecule, which allows them to be adsorbed on the metal surface. [1-2].

* Corresponding author: sweetdamself08@gmail.com

However, traditional inhibitors that contain toxic chemicals have raised environmental concerns and led to the search for alternative, sustainable solutions [2,3]. Natural products have been explored as potential inhibitors due to their eco-friendliness and abundance [4]. One such natural product is avocado seed. According to Villarreal-Lara et al. [5], the seeds are a significant waste product of avocado manufacturing, accounting for about 8-25% of the fruit's overall weight. Every year, about three hundred thousand loads of unwanted avocado seeds are generated, and because of the avocado seeds' availability and limited biodegradability, it is difficult to manage such waste. The various routes have been investigated to recognize other uses of avocado seeds and develop commercially viable products [5]. Hence, the seed has been found to contain anti-corrosive properties [5,6]. Gusti et al. [7] used methanol derived from avocado seeds in a sulfuric acid medium to shield the mild steel against corrosion. The authors (Gusti et al.) examined avocado seeds for potential use as mild steel corrosion inhibitors in 0.75 M H₂SO₄ acid medium. According to their findings, the inhibition efficiency was 74.56% via the weight loss technique, and with the potentiometric polarization technique 68.38% was attained at a 10 g / L concentration of avocado seed extract. It was further stated that the corrosion inhibition efficiency improved as the avocado seed extract's concentration increased. In another study, the effectiveness of avocado seed powder as a corrosion inhibitor for SAE 1008 carbon steel in acid media (0.5 mol/L HCl) was investigated by de Jesus et al. [8], milling and sifting at 170 mesh yielded the avocado seed powder. In HCl solution, different amounts of avocado seed powder were added. The findings from these experiments indicate that as the concentration of the avocado seed inhibitor increases, it exhibits a propensity to suppress corrosion. This suggests that the inhibitor is an effective agent for mitigating corrosive processes on the surface of steel [9].

Nonetheless, the study of avocado seed nanoparticles has been limited in their use as an inhibitor for steel, such as API X65, normally used for pipelines in the oil and gas industry [7, 8].

In the past years, RSM has gained popularity as a statistical technique for optimization in various fields, including chemistry and engineering [10]. RSM provides an efficient and cost-effective approach to optimize multiple process variables simultaneously and determine the optimum conditions for the desired outcome [11]. In the context of inhibitor optimization, RSM can be applied to determine the impact of various process variables on the inhibition efficiency of natural products [12], such as avocado seed nanoparticle extract.

Hence, this study investigated the optimum inhibition process variables of ASNE on API X65 steel using RSM. The influence of temperature, time, and concentration on the inhibition efficiency of ASNE were considered using a CCD to examine the optimal parameters for the inhibition process. The outcomes of this research provided valued insights into the use of ASNE as an inhibitor for API X65 steel and demonstrate the effectiveness of RSM in optimizing the inhibition process variables. Furthermore, the study will contribute to the growing body of knowledge on natural product-based inhibitors, which can serve as a sustainable alternative to traditional inhibitors in the gas and oil industry.

2 Materials and methodology

2.1 Syntheses of avocado seed nanoparticles

The ground avocado seed (AS) was obtained from a nearby farmstead in Pretoria, Gauteng, South Africa. The purchased avocado seed was washed, cleaned, and rinsed with distilled water. They were then dehydrated by drying in a low-temperature oven. Gbadeyan et al. [13] describe a combination of mechanical and chemical approaches for producing nanoparticles. The dry AS was first ground in a ball milling machine. The crushed powder

was then sieved mechanically to achieve the initial particle size of 50 μm. Furthermore, 50 g of AS powder was mixed with 200 mL of ethanol, and the mixture was wet milled for 4 hours before being allowed to settle for 48 hours. The clear liquid layer was then removed using the decantation technique to separate fine particle and solvent combinations. To ensure full solvent removal, the settling particles were washed with distilled water and separated using the decantation procedure. This operation was repeated five times to guarantee the cleanliness of the small particles. The obtained nanoparticles in the size range of 100-200nm were then dried in an oven at 350°C for 72 hours.

2.2 Preparation of solution and sample

Steel pipeline of grade API 5L X65 with chemical compositions, as shown in Table 1, was applied. The specimen were mechanically cut into 1 cm x 1 cm x 0.5 cm dimensions with the Struers Discotum-2 cut-off machine and the Corundum cut-off wheel. It was then ground again, carefully polished with grit silicon carbide sheets ranging in size from 240 μm to 1200 μm, degreased with ethanol, washed with distilled water, air dried, and stored in a desiccator. The corrosive solution was created by diluting 1M HCl acid from 37% analytical grade HCl with distilled water, which was used throughout the studies to prepare the solutions. Avocado seed nanoparticles extract (ASNE) weighing 1,2,3,4,5 g were then dissolved in 250ml of the stock solution, which was used as the corrosive environment for gravimetric tests. For every experiment, a newly prepared test medium was applied.

Table 1. Chemical compositions of API 5L X65 pipeline steel

| <i>Element</i> | <i>C</i> | <i>Si</i> | <i>P</i> | <i>Mn</i> | <i>Cu</i> | <i>Ni</i> | <i>S</i> | <i>Nb</i> | <i>Al</i> | <i>Fe</i> |
|-------------------|----------|-----------|----------|-----------|-----------|-----------|----------|-----------|-----------|-----------|
| Constituent (wt%) | 0.09 | 0.184 | 0.006 | 0.866 | 0.01 | 0.016 | 0.003 | 0.023 | 0.016 | Balance |

2.3 Weight loss corrosion test

The initial weight of individual samples was taken and recorded. Afterwards, the corrosive medium was prepared via the dilution of distilled water with a specific acid grade. This was used throughout the experiments for the medium preparation; this was achieved by separately diluting the acid with distilled water. A specific quantity was taken from the inhibitor solution and then directly added to the harsh media for varied concentrations prepared. Thus, the inhibitive features of the corrosion inhibitors on steel pipeline in the harsh solution were evaluated according to the ASTM G3 standard via the equations stated below [14].

$$Cr = \frac{87.6\Delta W}{DAT} \dots\dots\dots (1)$$

$$IE = \frac{Cr(\text{blank}) - Crh}{Cr(\text{blank})} \times 100 \% \dots\dots\dots (2)$$

Where, ΔW --- Weight loss in mg; A --- Area of sample in cm²; D is specimen density in g/cm³; T --- time in hours, Crh and Cr (blank) ---- depict the corrosion rate with and without ASN as an inhibitor, respectively.

2.4 Surface morphology study

The morphological study of the specimens was achieved by SEM equipped with EDX. The test samples were cleaned and prepared as specified in the sample preparation above.

The cut samples were soaked in 1 M HCl acid in the absence and presence of an inhibitor (1 – 5 g). The soaked samples were removed, rinsed, and oven dried. Subsequently, the samples' surfaces were examined with SEM to determine their morphology and phases, while EDX was applied to determine the elemental constituent.

3 Results and discussion

The outcomes obtained from the experiments conducted to optimize the inhibition process variables of ASNE on API X65 steel using response surface methodology (RSM) are presented and discussed below:

3.1 Gravimetric test

Figures 1-3 depict respectively the plot of weight loss, corrosion rate, and inhibition efficiency against time and concentration. Figure 1 reveals the performance of weight loss versus temperature and time. From the plots, the samples' weight loss increased from 0 – 20.8 mg when the exposure time increased from 24 – 480 hours. Whereas the inhibitor concentration increased from 1 – 5 g, there was a corresponding decrement in weight loss. Figure 2 shows that the inhibition efficiency increases with an increment in concentration. However, the inhibition efficiency declines with an exposure time increment. A synonymous outcome was achieved for plotting the corrosion rate versus time and concentration (Figure 3).

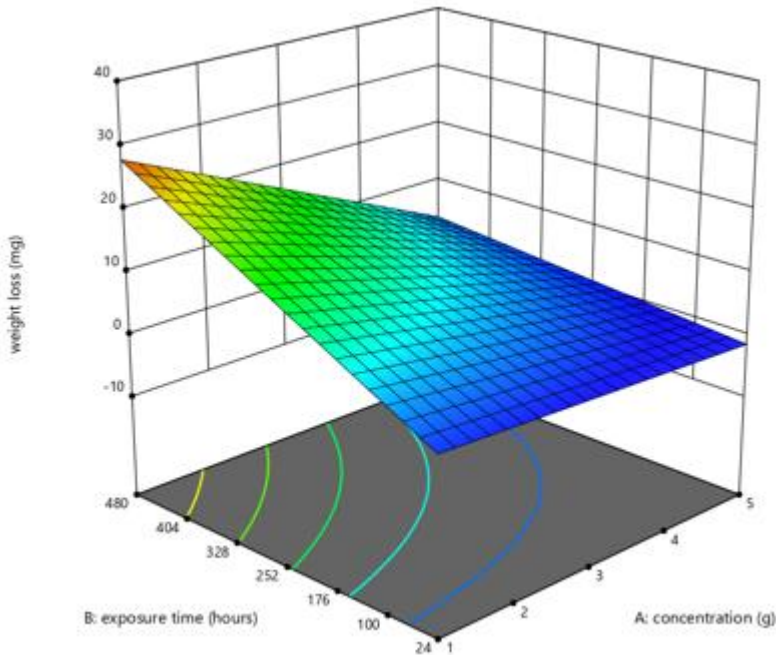


Fig. 1. The influence of concentration and time on the Weight loss of API steel pipeline.

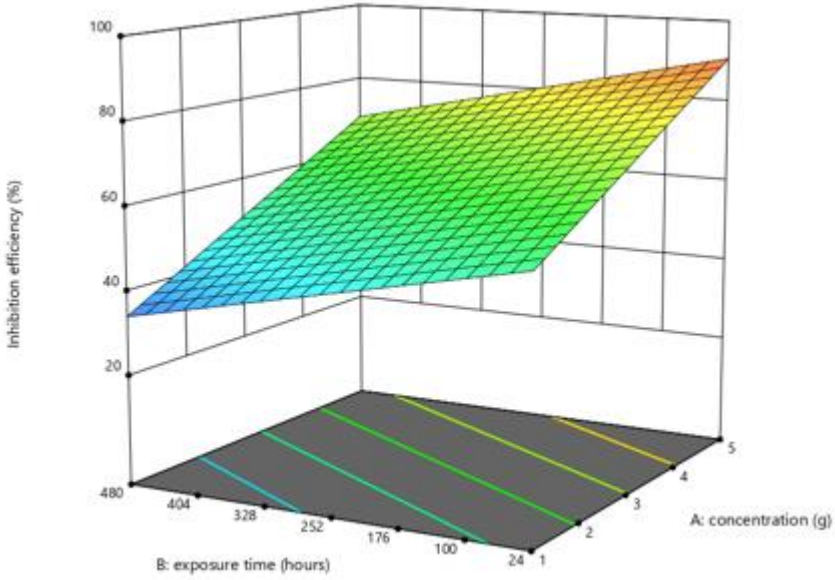


Fig. 2. The influence of concentration and time on the inhibition efficiency of API steel pipeline.

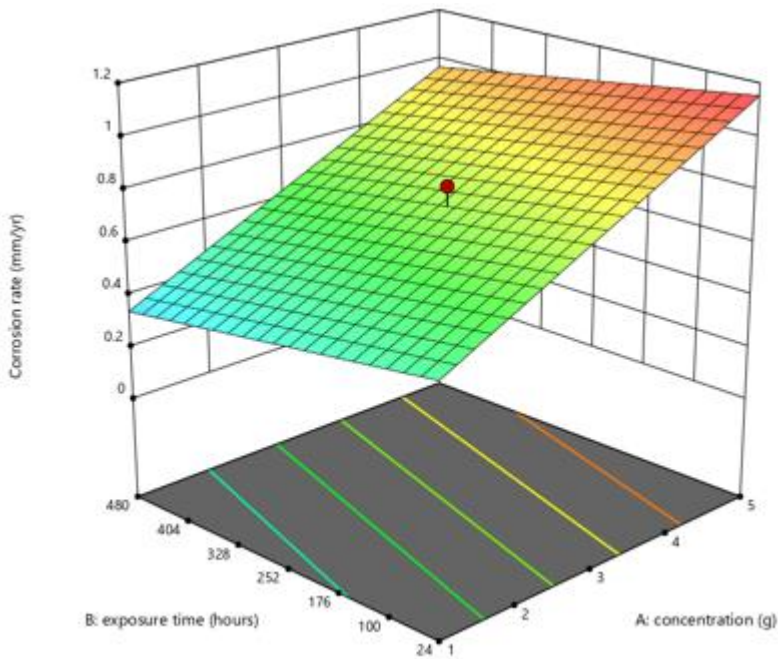


Fig. 3. The influence of concentration and time on the corrosion rate of API steel pipeline.

3.2 Design of experiment

The influence of temperature, concentration, and duration on the inhibitory effectiveness of ASNE were studied using a central composite design (CCD). Temperature (25-65°C), concentration (1-5 g), and duration (24-480 hours) were among the factors investigated. Only relevant variables were reported, allowing for a reduction in the number of tests performed, which was highly cost-effective and beneficial in determining the best answers using a second-order quadratic polynomial equation, as shown in Equations 3 and 4. Stat-Ease Inc. Design Expert Software 11 was used to evaluate the statistical data.

$$Y = \beta_0 + \sum_{i=1}^k \beta_i A_i + \sum_{i=1}^k \beta_{ii} A_i^2 + \sum_{i=1}^k \sum_{j=1}^k \beta_{ij} A_i A_j + \varepsilon \dots\dots\dots (3)$$

$$Y = \beta_0 + \beta_i A_i + \beta_{ii} A_i^2 + \beta_{jk} A_j A_k \dots\dots\dots (4)$$

A_i , B_{ij} and AB_k are the significant terms of the independent variable in the regression model, the response output is Y , and the intercept constant is β_0 . The regression coefficients are β_i , β_{ii} , β_{jk} and β_{ij} while the experimental errors are represented by ε .

The collated experimental data were analyzed via RSM to discover the best settings for the inhibition mechanism variables. The investigation included fitting a second-order polynomial model to the experimental data and utilizing analysis of variance (ANOVA) to determine the important variables. Based on the maximum inhibition effectiveness, the best parameters for the inhibition process were found. The optimum conditions for the inhibition efficiency were confirmed experimentally and compared to the predicted value.

Table 3 shows the model's F-value of 37.26, indicating that it is significant. An F-value this big could be developed because of noise just 0.01% of the time. Model terms with P-values below 0.0500 are significant. Hence, in this scenario, the important model terms are A, B, and C.

Table 2. DOE result of the corrosion inhibition of API X65 in 1M HCl by ASNE.

| Std | Run | Factor 1 A: Concentration (g) | Factor 2 B: Exposure Time (hours) | Factor 3 C: Temperat ure (°C) | Response 1 Weight loss (mg) | Response 2 Corrosion rate (mm/yr) | Response 3 Inhibition efficiency (%) |
|-----|-----|--|---|---|--------------------------------------|---|--|
| 13 | 1 | 3 | 240 | 45 | 4.8 | 0.82764 | 61.4351 |
| 5 | 2 | 1 | 24 | 65 | 3.4 | 0.681302 | 45.76 |
| 9 | 3 | 3 | 240 | 45 | 4.8 | 0.82764 | 61.4351 |
| 8 | 4 | 5 | 480 | 65 | 6.2 | 1.10553 | 66.8234 |
| 4 | 5 | 5 | 480 | 25 | 4.1 | 0.855124 | 76.9231 |
| 2 | 6 | 5 | 24 | 25 | 0.1 | 0.956522 | 95.6522 |
| 11 | 7 | 3 | 240 | 45 | 4.8 | 0.82764 | 61.4351 |
| 1 | 8 | 1 | 24 | 25 | 2.3 | 0.391304 | 68.75 |
| 3 | 9 | 1 | 480 | 25 | 28.3 | 0.138393 | 39.4211 |
| 7 | 10 | 1 | 480 | 65 | 30.6 | 0.33845 | 28.2341 |
| 6 | 11 | 5 | 24 | 65 | 0.4 | 1.13467 | 85.3456 |
| 12 | 12 | 3 | 240 | 45 | 4.8 | 0.82764 | 61.4351 |
| 10 | 13 | 3 | 240 | 45 | 4.8 | 0.82764 | 61.4351 |

Table 3. ANOVA for Linear Model Corrosion Rate

| Source | Sum of Squares | df | Mean Square | F-value | p-value | |
|------------------|----------------|----|-------------|---------|----------|-------------|
| Model | 0.9579 | 3 | 3 | 37.26 | < 0.0001 | significant |
| A-concentration | 0.7827 | 1 | 1 | 91.34 | < 0.0001 | |
| B-exposure time | 0.0697 | 1 | 1 | 8.13 | 0.0191 | |
| C-temperature | 0.1055 | 1 | 1 | 12.31 | 0.0066 | |
| Residual | 0.0771 | 9 | 9 | | | |
| Lack of Fit | 0.0771 | 5 | 5 | | | |
| Pure Error | 0.0000 | 4 | 4 | | | |
| Cor Total | 1.04 | 12 | | | | |

Table 4 shows the model's F-value of 127.76, indicating that the model is significant. An F-value this big could be developed because of noise just 0.01% of the time. Model terms with P-values below 0.05 are significant. Hence, in this scenario, the important model terms are A, B, and C. The values beyond 0.1 indicate the unimportance of the model term. The model reduction can be applied to enhance a model if there are numerous unimportant model terms (excluding those necessary to assist hierarchy).

Table 4. ANOVA for Linear Model Inhibition Efficiency.

| Source | Sum of Squares | df | Mean Square | F-value | p-value | |
|------------------|----------------|----|-------------|---------|----------|-------------|
| Model | 3790.26 | 3 | 1263.42 | 127.76 | < 0.0001 | significant |
| A-concentration | 2541.10 | 1 | 2541.10 | 256.95 | < 0.0001 | |
| B-exposure time | 876.74 | 1 | 876.74 | 88.65 | < 0.0001 | |
| C-temperature | 372.42 | 1 | 372.42 | 37.66 | 0.0002 | |
| Residual | 89.00 | 9 | 9.89 | | | |
| Lack of Fit | 89.00 | 5 | 17.80 | | | |
| Pure Error | 0.0000 | 4 | 0.0000 | | | |
| Cor Total | 3879.26 | 12 | | | | |

Table 5 reveals the model's F-value of 20.36, indicating that it is significant. An F-value this big could be developed because of noise just 0.10% of the time. The model terms with P-values below 0.05 are significant. Hence, in this scenario, the important model terms are A, B, and AB.

Table 5. ANOVA for Linear Model Weight Loss.

| Source | Sum of Squares | df | Mean Square | F-value | p-value | |
|--------------|----------------|----|-------------|---------|---------|-------------|
| Model | 1110.16 | 6 | 185.03 | 20.36 | 0.0010 | significant |

| | | | | | | |
|------------------|---------|----|--------|--------|--------|--|
| A-concentration | 361.81 | 1 | 361.81 | 39.81 | 0.0007 | |
| B-exposure time | 507.45 | 1 | 507.45 | 55.83 | 0.0003 | |
| C-temperature | 4.20 | 1 | 4.20 | 0.4626 | 0.5218 | |
| AB | 235.44 | 1 | 235.44 | 25.90 | 0.0022 | |
| AC | 0.1250 | 1 | 0.1250 | 0.0138 | 0.9105 | |
| BC | 1.13 | 1 | 1.13 | 0.1238 | 0.7370 | |
| Residual | 54.54 | 6 | 9.09 | | | |
| Lack of Fit | 54.54 | 2 | 27.27 | | | |
| Pure Error | 0.0000 | 4 | 0.0000 | | | |
| Cor Total | 1164.69 | 12 | | | | |

The ANOVA showed that all three variables, concentration, temperature, and time, significantly affected the inhibition efficiency of ASNE on API X65 steel ($p < 0.05$). The coefficient of determination (R^2) value of the model was 0.983, indicating that the model could clarify 98.3% of the variability in the inhibition efficiency of ASNE.

The optimization process determined the optimal parameters for the inhibition mechanism variables to be 40 °C, at a concentration of 5 g/L, and a time of 24 hours. The predicted inhibition efficiency at these optimum conditions was 96.7%, and the experimental validation of the predicted value resulted in an inhibition efficiency of 96.5%, approximately near the predicted value, as depicted in Figure 4.

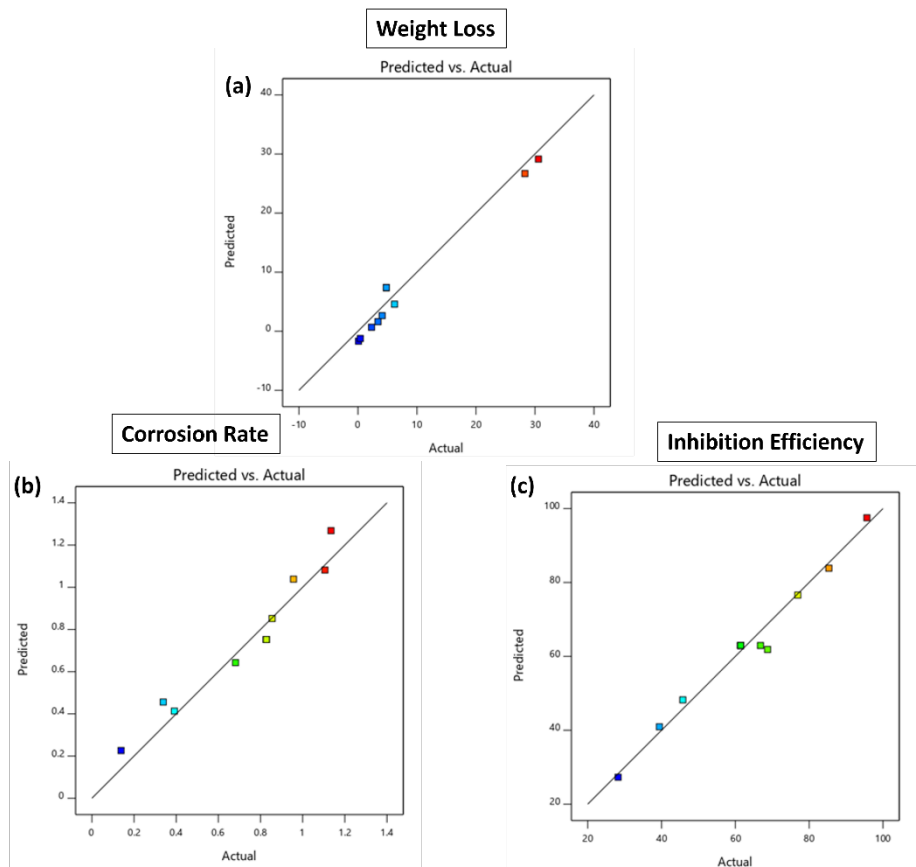


Fig. 4. Predicted vs. Actual Data Graph (a) Weight loss, (b) Corrosion Rate, and (c) Inhibition Efficiency.

The optimized conditions of temperature, concentration, and time were found to agree with the literature, which reported that a higher temperature and inhibitor concentration could increase the inhibition efficiency [13-17]. However, the graphs also showed that with an increase in time beyond a certain point apparently did not increase the inhibition efficiency. This finding is important as it can aid in declining the inhibition process cost by minimizing the time required for the inhibition process. Hence, the high inhibition efficiency of ASNE on API X65 steel can be attributed to the presence of nanoparticles form of the extract, which adsorbs onto the steel surface to develop a protective layer.

3.3 Surface analysis

The SEM/EDX evaluation of the experimented samples after corrosion examination is revealed in Figures 5-6. Figure 6 reveals the impact of optimum processing parameters on the surface of the sample, which further elucidates the build-up of ASNE as shown by the EDX. The detected agglomeration of the particles with inhibitor on the surface got

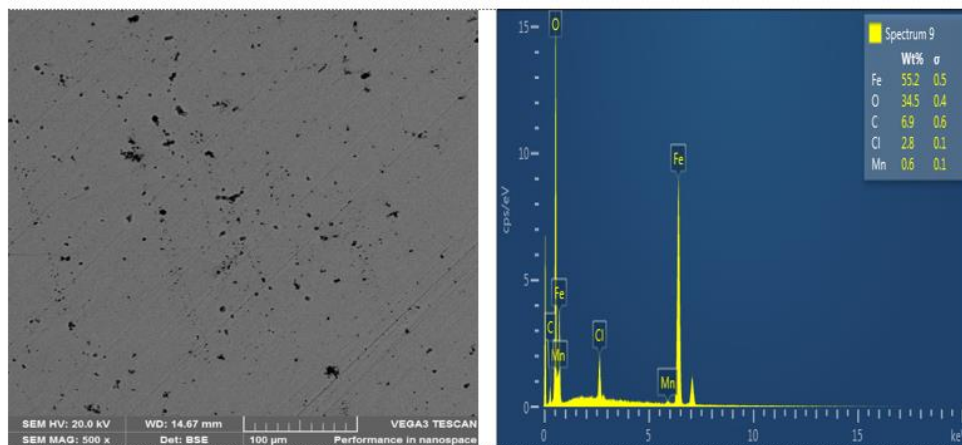


Fig. 5. SEM/EDX of API X65 in 1M HCl acid solution without the addition of ASNE after 480 hours.

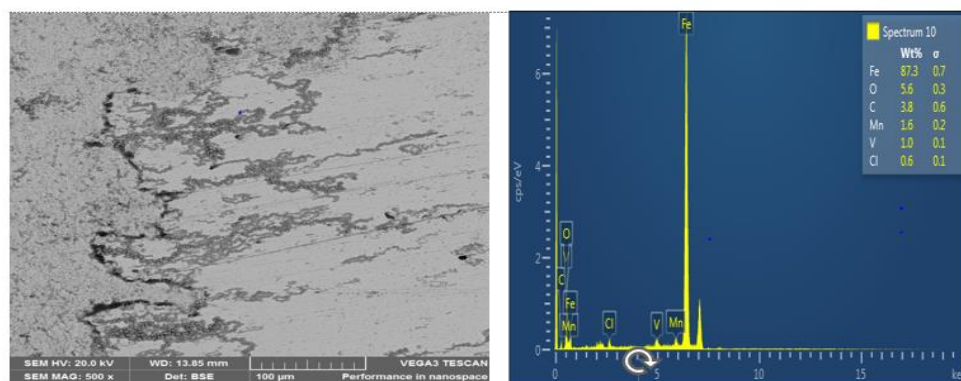


Fig. 6: SEM/EDX of API X65 in 1M HCl acid solution with the addition of ASNE after 480 hours.

increased because of the improved powder composition union, resulting in a densified structure with minimized corrosion rate. Figure 5, the blank sample revealed grubby film and micro-cracks in their damaged surface. This is owed to the lack of shielding film in the acidic solution, which produced a rise in the corrosion rate. The augmented cracks and deformation observed on the sample in the absence of an inhibitor are ascribed to the corrosive nature of the solution. The results obtained from SEM/EDX analysis can be interpreted in conjunction with the observed trend depicted in the 3D surface graphs (Figures 1-3). These graphs illustrate that the inhibition efficiency exhibited a linear improvement as the concentration of the inhibitor increased. At high concentrations of the ASNE inhibitor, a greater extent of surface area is covered due to adsorption, resulting in the reduction of corrosive active sites. Consequently, this leads to a decrease in the rate of corrosion and an enhancement in the efficiency of inhibition. This result demonstrated a comparable outcome to that of Van der Ven et al. [12]. Figure 5 also illustrates the elemental constituent of the uninhibited sample that exhibited a significant presence of chlorine (Cl) and oxygen (O). The observed result may be ascribed to the impact of the aggressive solution and the subsequent development of corrosion by products on the steel substrate. Additionally, the analysis revealed low levels of oxygen (O) and chlorine (Cl) content, indicating that ASNE serves as a protective agent, preventing the adsorption of Cl and O atoms on the steel surface. This indicates that the inclusion of ASNE in the acidic solution contributes to the protection of the metal. Also, the introduction of ASNE inhibitor resulted in a gradual increase in the Fe atom ratio and a

gradual decrease in the O atom concentration on the surface of X65 steel. This finding can be attributed to the interaction between O₂ and the Fe³⁺ bond present in Fe₂O₃ and Fe₃O₄ [17].

4 Conclusion

In conclusion, this study successfully optimized the inhibition process variables of ASNE on API X65 steel using RSM. The optimal parameters for the inhibition mechanism were established to be at a temperature of 25 °C, a concentration of 5 g/L, and a time of 24 hours, resulting in an inhibition efficiency of 96.7%. The scanning electron microscopy (SEM) analysis reveals that the inhibited sample exhibits a more effectively protected surface compared to the uninhibited sample under the optimal inhibiting parameter. This enhanced protection can be attributed to the presence of the ASNE inhibitor, which acts as a protective shield on the metal surface. The study provides valuable insights into using natural product-based inhibitors and demonstrates the effectiveness of response surface methodology in optimizing the inhibition process variables.

Acknowledgements

The authors appreciate the Surface Engineering Research Laboratory (SERL) at Tshwane University of Technology, Pretoria, for their Laboratory equipment and official assistance.

Reference

1. Hasson, D., Shemer, H. and Sher, A. 2011. State of the art of friendly “green” scale control inhibitors: a review article. *Industrial & Engineering Chemistry Research*, 50(12), pp.7601-7607.
2. Salminen, A., Lehtonen, M., Suuronen, T., Kaarniranta, K. and Huuskonen, J. 2008. Terpenoids: natural inhibitors of NF-κB signaling with anti-inflammatory and anticancer potential. *Cellular and Molecular Life Sciences*, 65, pp.2979-2999.
3. Verma, C., Alfantazi, A., Quraishi, M.A. and Rhee, K.Y. 2023. Are extracts really green substitutes for traditional toxic corrosion inhibitors? Challenges beyond origin and availability. *Sustainable Chemistry and Pharmacy*, 31, p.100943.
4. Raja, P.B. and Sethuraman, M.G. 2008. Natural products as corrosion inhibitor for metals in corrosive media—a review. *Materials Letters*, 62(1), pp.113-116.
5. Villarreal-Lara, R., Rodríguez-Sánchez, D.G., Díaz De La Garza, R.I., García-Cruz, M.I., Castillo, A., Pacheco, A. and Hernández-Brenes, C. 2019. Purified avocado seed acetogenins: Antimicrobial spectrum and complete inhibition of *Listeria monocytogenes* in a refrigerated food matrix. *CyTA-Journal of Food*, 17(1), pp.228-239.
6. Charles, A.C., Dadmohammadi, Y. and Abbaspourrad, A. 2022. Food and cosmetic applications of avocado seed: a review. *Food & Function*, 13, pp.6894-6901.
7. Gusti, D.R., Lestari, I., Farid, F. and Sirait, P.T. 2019. Protection of mild steel from corrosion using methanol extract of avocado (*Persea americana* mill) seeds in a solution of sulfuric acid. In *Journal of Physics: Conference Series*, 1282(1), pp. 012083). IOP Publishing.
8. de Jesus, M. E. S., de Mendonça Santos, A., Tokumoto, M. S., Cotting, F., Aquino, I. P., & Capelossi, V. R. (2020). Evaluation of Efficiency of avocado seed powder (*Persea*

- Americana) as a corrosion inhibitor in SAE 1008 carbon steel in acidic medium. *Brazilian Journal of Development*, 6(10), 77197-77215.
9. Cruz-Zabalegui, A., Vazquez-Velez, E., Galicia-Aguilar, G., Casales-Diaz, M., Lopez-Sesenes, R., Gonzalez-Rodriguez, J.G. and Martinez-Gomez, L. 2019. Use of a non-ionic gemini-surfactant synthesized from the wasted avocado oil as a CO₂-corrosion inhibitor for X-52 steel. *Industrial Crops and Products*, 133, pp.203-211.
 10. Khuri, A.I. and Mukhopadhyay, S. 2010. Response surface methodology. *Wiley Interdisciplinary Reviews: Computational Statistics*, 2(2), pp.128-149.
 11. Dean, A., Voss, D., Draguljić, D., Dean, A., Voss, D. and Draguljić, D. 2017. Response surface methodology. *Design and analysis of experiments*, pp.565-614.
 12. Van der Ven, C., Gruppen, H., de Bont, D.B. and Voragen, A.G. 2002. Optimization of the angiotensin-converting enzyme inhibition by whey protein hydrolysates using response surface methodology. *International Dairy Journal*, 12(10), pp.813-820.
 13. Gbadeyan, O. J., Adali, S., Bright, G., & Sithole, B. (2022). Comparative reinforcement effect of *Achatina fulica* Snail shell nanoparticles, montmorillonite, and kaolinite nanoclay on the mechanical and physical properties of greenpoxy biocomposite. *Polymers*, 14(3), 365.
 14. Hemapriya, V., Prabakaran, M., Chitra, S., Swathika, M., Kim, S.H. and Chung, I.M, 2020. Utilization of biowaste as an eco-friendly biodegradable corrosion inhibitor for mild steel in 1 mol/L HCL solution. *Arabian Journal of Chemistry*, 13(12), pp8684-8696
 15. Farhadian, A., Rahimi, A., Safaei, N., Shaabani, A., Abdouss, M. and Alavi, A. 2020. A theoretical and experimental study of castor oil-based inhibitor for corrosion inhibition of mild steel in acidic medium at elevated temperatures. *Corrosion Science*, 175, p.108871.
 16. Noor, E.A. and Al-Moubaraki, A.H. 2008. Thermodynamic study of metal corrosion and inhibitor adsorption processes in mild steel/1-methyl-4 [4'(-X)-styryl pyridinium iodides/hydrochloric acid systems. *Materials Chemistry and Physics*, 110(1), pp.145-154
 17. Bahru, T.B., Tadele, Z.H. and Ajebe, E.G. 2019. A review on avocado seed: functionality, composition, antioxidant and antimicrobial properties. *Chemical Science International Journal*, 27(2), pp.1-10